Steady helix states in a resonant XXZ Heisenberg model with Dzyaloshinskii-Moriya interaction

E. S. Ma ⬤, K. L. Zhang ⬤, and Z. Song ⬤*

School of Physics, Nankai University, Tianjin 300071, China

We systematically investigate possible helix states in the XXZ Heisenberg model with the Dzyaloshinskii-Moriya (DM) interaction. Exact solutions show that a set of precession helix states can be constructed by deliberate superposition of degenerate eigenstates of the Hamiltonian under the resonant condition. When a non-Hermitian balance boundary term is imposed as a quenching action, the quench dynamics shows that a steady helix state emerges from some easily prepared initial states, including saturated and maximally mixed ferromagnetic states, according to the analysis of the perturbation method. The corresponding dynamics for near resonant cases is also investigated numerically, indicating the robustness of the scheme. Our findings highlight the cooperation of non-Hermiticity and the DM interaction in a quantum spin system, suggesting a way for preparing a steady helix state in a non-Hermitian quantum spin system.

I. INTRODUCTION

The quantum Heisenberg model, as a simple model of interacting spins, takes an important role in physics. It not only captures the properties of many magnetic materials but also provides a tractable theoretical example for understanding fundamental concepts in physics. Although the one-dimensional Heisenberg chain is an old topic, quantum dynamics of the system is still an active frontier of research, especially after the quantum simulator has been realized in experiments [1–7]. Recently, the discovery of highly excited many-body eigenstates of the Heisenberg model, referred to as Bethe phantom states, has received much attention from both theoretical [8–11] and experimental approaches [12–15].

In this paper, we investigate possible helix states in the XXZ Heisenberg model under two considerations. One corresponds to the introduction of Dzyaloshinskii-Moriya (DM) interaction. The DM interaction is an antisymmetric exchange interaction that appears in inversion asymmetric structures and favors perpendicular alignment of neighboring spins in a magnetic material [16–18]. In materials with inversion symmetry, the frustration interaction [19,20] can also cause a helix ground state [21–24]. The other is the imposed non-Hermitian balance boundary condition, which takes the role of the source and drain of a spin flip. Under a resonant condition on the DM and anisotropic terms, the modified Heisenberg model obeys the SU(2) symmetry, and then possesses a set of degenerate eigenstates. It allows the existence of a spin helix state as an exact solution obtained by deliberate superposition of these degenerate eigenstates. We are mainly interested in the dynamic preparation of the spin helix state. Based on the analysis of the perturbation method, it is shown that a steady helix state emerges from some easily prepared initial states, including saturated and maximally mixed ferromagnetic states, when a non-Hermitian balance boundary is imposed as a

quenching action. For near resonant cases, the corresponding dynamics is also investigated numerically, and the results indicate that the scheme works well at a certain time window. It relates to an exclusive concept in a non-Hermitian system, the exceptional point (EP), which has no counterpart in a Hermitian system. The EP in a non-Hermitian system occurs when eigenstates coalesce [25–27] and is usually associated with the non-Hermitian phase transition [28,29]. In a parity-time ($\mathcal{PT}$)-symmetric non-Hermitian coupled system, the $\mathcal{PT}$ symmetry of eigenstates spontaneously breaks at the EP [30–35], which determines the exact $\mathcal{PT}$-symmetric phase and the broken $\mathcal{PT}$-symmetric phase in this system.

We will impose a pair of balance non-Hermitian impurities [36,37] to the ends of the spin chain as the non-Hermitian boundary condition. The corresponding dynamics is also investigated analytically and numerically. The approximate solutions for the quantum spin chain with finite length provide valuable insights for the description of the nonequilibrium dynamics. Our findings highlight the cooperation of non-Hermiticity and the DM interaction in a quantum spin system, suggesting a way for preparing a steady helix state in a non-Hermitian quantum spin system.

The rest of this paper is organized as follows: In Sec. II, we introduce the model Hamiltonian and the corresponding SU(2) symmetry. With these preparations, in Sec. III, we demonstrate that two types of helix states can be constructed by a set of degenerate eigenstates. Based on these results, the dynamic generation of a spin helix state is proposed in Sec. IV by means of three kinds of imposed fields. Section V concludes this paper.

II. MODEL HAMILTONIAN AND SYMMETRIES

We begin this section by introducing a general Hamiltonian:

$$H = H_0 + H_I, \tag{1}$$

*songtc@nankai.edu.cn

where H_0 and H_I describe a quantum spin Heisenberg chain with a DM interaction and an external interaction, respectively:

$$
H_0 = -\sum_{j=1}^{N-1} \left(J_x s_j^x s_{j+1}^x + J_y s_j^y s_{j+1}^y + J_z s_j^z s_{j+1}^z \right)
$$
$$
+ i\frac{D}{2} \sum_{j=1}^{N-1} \left(s_j^+ s_{j+1}^- - s_j^- s_{j+1}^+ \right), \tag{2}
$$

$$
H_I = \sum_{j=1}^{N} \mathbf{B}_j \cdot \mathbf{s}_j. \tag{3}
$$

Here, $\mathbf{s}_j = (s_j^x, s_j^y, s_j^z)$ is the spin-$\frac{1}{2}$ operator, and $\mathbf{B}_j$ is the onsite magnetic field inducing Hermitian or non-Hermitian impurity. In this paper, we only focus on the case with $J_x = J_y$, and by taking $(J_x)^2 + D^2 = 1$ and $\Delta = J_z$ for the sake of simplicity, we rewrite H_0 in the form [38]:

$$
H_0 = -\sum_{j=1}^{N-1} \left[\frac{\exp(-ik_0)}{2} s_j^+ s_{j+1}^- + \frac{\exp(ik_0)}{2} s_j^- s_{j+1}^+ \right.
$$
$$
\left. + \Delta s_j^z s_{j+1}^z \right], \tag{4}
$$

Comparing with the XXZ Heisenberg model without a DM interaction, there are two additional phase factors $\exp(-ik_0)$ and $\exp(ik_0)$, where $k_0 = \arctan(D/J_x)$ is a crucial factor for the helix state arising from D. For arbitrary Δ, we always have

$$
[s^z, H_0] = 0, \tag{5}
$$

with $s^z = \sum_{j=1}^{N} s_j^z$. Importantly, for the resonant case with $\Delta = 1$ defining

$$
s_{k_0}^+ = \left(s_{k_0}^- \right)^\dagger = \sum_{j=1}^{N} \exp(ik_0 j) s_j^+, \tag{6}
$$

we have

$$
\left[s_{k_0}^\pm, H_0 \right] = 0, \tag{7}
$$

which is not a surprising result since $s_{k_0}^\pm$ and s^z satisfy the Lie algebra commutation relations:

$$
\left[s_{k_0}^+, s_{k_0}^- \right] = 2s^z, \quad \left[s^z, s_{k_0}^\pm \right] = \pm s_{k_0}^\pm. \tag{8}
$$

It seems a little trivial but is helpful for the following processing in the presence of impurity term H_I.

III. TWO TYPES OF HELIX STATES

In this section, we will introduce two types of helix states based on the eigenstates of H_0 with $\Delta = 1$. We start by the ferromagnetic eigenstate of H_0:

$$
|\psi_0\rangle = |\Downarrow\rangle = \prod_{j=1}^{N} |\downarrow\rangle_j, \tag{9}
$$

satisfying the equation $H_0|\psi_0\rangle = -(N-1)/4|\psi_0\rangle$, with $s_j^z|\downarrow\rangle_j = -\frac{1}{2}|\downarrow\rangle_j$. Based on the symmetry of H_0 mentioned

above, a set of eigenstates $\{|\psi_n\rangle, n \in [1, N]\}$ can be constructed as

$$
|\psi_n\rangle = \frac{1}{\Omega_n} \left(s_{k_0}^+ \right)^n |\Downarrow\rangle, \tag{10}
$$

where the normalization factor $\Omega_n = (n!)\sqrt{C_N^n}$. Obviously, we have $|\psi_N\rangle = \exp[ik_0(1+N)N/2]|\Uparrow\rangle = \exp[ik_0(1+N)N/2]\prod_{j=1}^{N}|\uparrow\rangle_j$. It can be verified that these degenerate states are ground eigenstates of H_0. We introduce a local vector $\mathbf{h}_l = (h_l^x, h_l^y, h_l^z)$ with $h_l^\alpha = \langle\psi|s_l^\alpha|\psi\rangle$ ($\alpha = x, y, z$) to characterize the helicity of a given state $|\psi\rangle$.

For eigenstates $|\psi_n\rangle$, straightforward derivation of $h_l^\alpha(n) = \langle\psi_n|s_l^\alpha|\psi_n\rangle$ show that

$$
h_l^x(n) = h_l^y(n) = 0, \quad h_l^z(n) = \frac{n}{N} - \frac{1}{2}, \tag{11}
$$

which is uniform, indicating that $|\psi_n\rangle$ is not a helix state. Nevertheless, in the following, we will show that their superposition can be helix states, and these states can be classified as two types of helix states: precession and entangled helix states.

A. Precession helix state

We consider a superposition eigenstate in the form:

$$
|\phi(\theta)\rangle = \sum_n d_n |\psi_n\rangle, \tag{12}
$$

where

$$
d_n = \sqrt{C_N^n} (-i)^n \sin^n\left(\frac{\theta}{2}\right) \cos^{(N-n)}\left(\frac{\theta}{2}\right). \tag{13}
$$

The corresponding helix vector is

$$
\mathbf{h}_l = \frac{1}{2}[\sin\theta \sin(k_0 l), \sin\theta \cos(k_0 l), -\cos\theta], \tag{14}
$$

which indicates that $|\phi(\theta)\rangle$ is a helix state for nonzero $\sin\theta$. Here, θ is an arbitrary angle and determines the profile of the state. This can be obtained easy when we express it in the form:

$$
|\phi(\theta)\rangle = \prod_{j=1}^{N} \left[-i\exp(ik_0 j)\sin\left(\frac{\theta}{2}\right)|\uparrow\rangle_j + \cos\left(\frac{\theta}{2}\right)|\downarrow\rangle_j \right]. \tag{15}
$$

It represents a tensor product of the precession states of all spins, which is a standard helix state. It is one of the physically interesting states that has been investigated both in theoretical and experimental aspects recently [9,11,15]. Obviously, such helix states are the ground eigenstates of H_0 with the condition $\Delta = 1$. In the XXZ Heisenberg model without a DM interaction, there also exists a helix state that is the eigenstate of the Hamiltonian but only for infinite N or for a finite system with the aid of appropriate boundary conditions [11]. The standard helix state accords with the result $|\mathbf{h}_l|^2 = \frac{1}{4}$. Plots of $\mathbf{h}_l$ for several typical cases are presented in Fig. 1.

In addition, one can express state $|\phi(\theta)\rangle$ in the form $|\phi(\theta)\rangle = R_\theta^+|\Downarrow\rangle$, where the operator is

$$
R_\theta^\pm = \sum_n \frac{d_n}{\Omega_n} \left(s_{k_0}^\pm \right)^n, \tag{16}
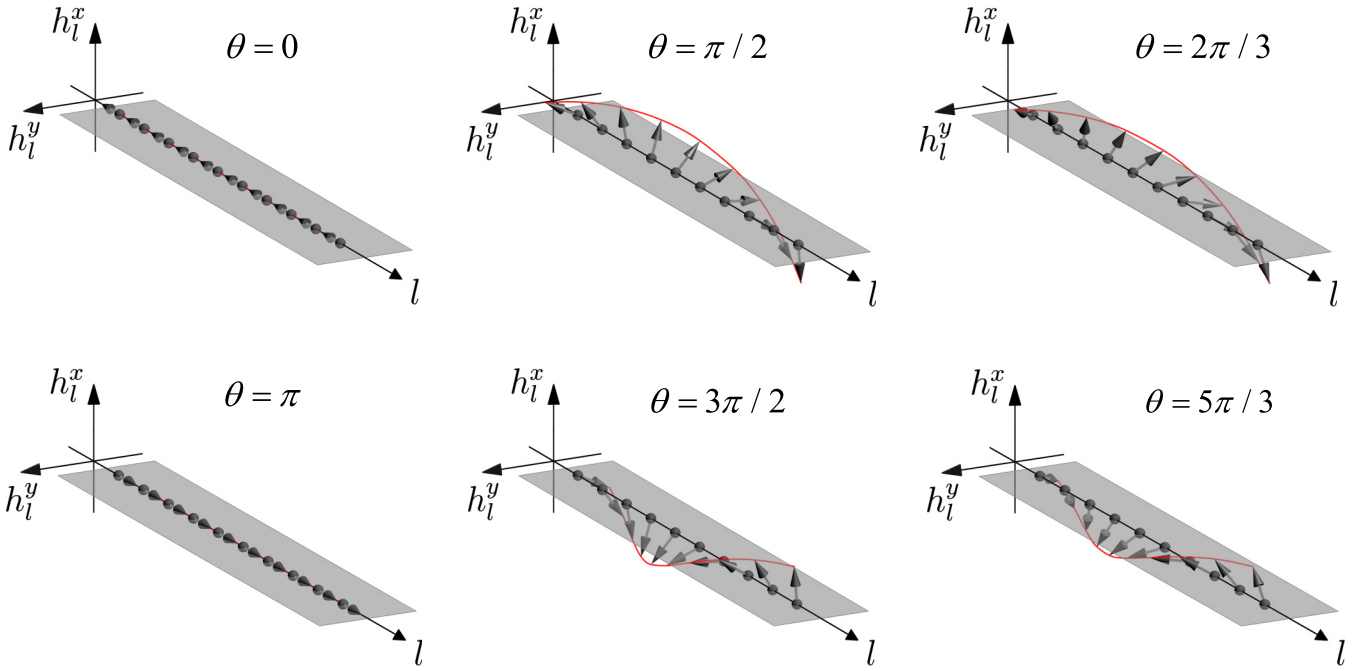$$

FIG. 1. Plots of helix vector from Eq. (12) for several representative values of θ, with parameters $k_0 = \arctan(0.5)$ and $N = 10$. For $\theta = 0$ and π, all spins align in the z direction. For $\theta = \pi/2$ and $3\pi/2$, all spins lie in the xy plane.

satisfying

$$\left[R_\theta^\pm, H_0 \right] = 0. \tag{17}$$

We note that

$$(R_\theta^+)^m |\phi(\theta)\rangle \propto |\phi(\theta')\rangle, \tag{18}$$

with $\tan(\theta'/2) = (m+1)\tan(\theta/2)$, which indicates that the action of operator $(R_\theta^+)^m$ is a shift of the angle $\theta \longrightarrow \theta'$, referred to as an angle shift operator.

B. Entangled helix state

In this paper, we are mainly concerned with the standard helix state; however, it is worth noting that there exists an entangled helix state in the system. Here is an example for an entangled helix state. We construct a state, which is just the superposition of the saturated ferromagnetic state and single-magnon states:

$$|\psi_E\rangle = \frac{1}{\sqrt{N^2 + N}} \sum_{j=1}^N \left[\exp(ik_0 j)s_j^+ + 1 \right] |\Downarrow\rangle. \tag{19}$$

The corresponding helix vector is

$$\mathbf{h}_l = \frac{1}{2(N+1)} \left[2\cos(k_0 l), -2\sin(k_0 l), \frac{2}{N} - N - 1 \right], \tag{20}$$

which indicates that $|\psi_E\rangle$ is a weak helix state for finite N. In addition, we note that

$$|\mathbf{h}_l|^2 = \frac{4N^2 + (N^2 + N - 2)^2}{4N^2(N+1)^2}, \tag{21}$$

and $|\mathbf{h}_l|^2 < \frac{1}{4}$ for finite N. It indicates that $|\psi_E\rangle$ cannot be written as a tensor product, in the form of $|\phi(\theta)\rangle$. Helix state $|\psi_E\rangle$ is an entangled state. This example indicates that, if the

coefficients $\{d'_n\}$ of superposition $\sum_n d'_n |\psi_n\rangle$ are deviated from the set $\{d_n\}$ a little, the quasihelix state is probably entangled.

In comparison with the helix states presented in previous work [11,15], the existence of the set of states $\{|\psi_n\rangle\}$ are well understood on the basis of the modified SU(2) symmetry of H_0. In the presence of H_I, the SU(2) symmetry is broken, $(N+1)$-fold degeneracy is left, and the set of states $\{|\psi_n\rangle\}$ is no longer the eigenstates. Nevertheless, certain appropriately designed external field H_I may provide a pathway to hybrid $(N+1)$-fold degenerate states, forming the helix state on demand. Like the helix state in the XXZ chain, the present helix states contain the information of H_0 and the strength of DM interaction D.

IV. DYNAMIC GENERATION OF HELIX STATE

In this section, we focus on the preparation of a helix state through a dynamic way, which is a crucial step in a coherent experimental protocol. The strategy is to take an easily prepared eigenstate of H_0 as the initial state and then add H_I. It is expected that the evolved state will be a helix state at a certain instant. In the following, we consider three kinds of H_I, which are spatially modulated Hermitian and non-Hermitian fields and a balanced non-Hermitian boundary, respectively.

A. Hermitian field

We consider the situation that the system is exerted by a resonant field:

$$\mathbf{B}_j = B_0(t)[\cos(k_0 j), -\sin(k_0 j), 0], \tag{22}$$

where $B_0(t)$ is an arbitrary function of time but is taken as a pulse function in our scheme. Here, the word *resonance* does not mean in the magnitude or frequency but the matching

distribution of the field with coupling strength in the spin chain. We will show that such a spatially modulated pulse field can drive a simple ferromagnetic state to a precession helix state.

In general, the time evolution of a given initial state $|\psi(0)\rangle$ under a time-dependent Hamiltonian $H(t)$ can be expressed as

$$|\psi(t)\rangle = \mathcal{T} \exp\left[-i\int_0^t H(t')dt'\right]|\psi(0)\rangle, \quad (23)$$

with $\mathcal{T}$ being the time-ordered operator. The merit of a resonant field is the commutative relation:

$$[H_0, H_I] = 0, \quad (24)$$

which ensures the analytical expression:

$$|\psi(t)\rangle = \exp\left[it\frac{N-1}{4}\right]\exp\left[-i\int_0^t H_I(t)dt\right]|\Downarrow\rangle$$

$$= \exp\left[it\frac{N-1}{4}\right]\prod_{j=1}^N$$

$$\times \left\{ -i\exp(ik_0 j)\sin\left[\int_0^t \frac{1}{2}B_0(t')dt'\right]|\uparrow\rangle_j \right.$$

$$\left. + \cos\left[\int_0^t \frac{1}{2}B_0(t')dt'\right]|\downarrow\rangle_j \right\}. \quad (25)$$

for the initial state $|\psi(0)\rangle = |\Downarrow\rangle$. Obviously, it is a precession helix state with the vector:

$$\mathbf{h}_l(t) = \tfrac{1}{2}[\sin\theta\sin(k_0 l), \sin\theta\cos(k_0 l), -\cos\theta], \quad (26)$$

where θ is a function of time:

$$\theta(t) = \int_0^t B_0(t')dt'. \quad (27)$$

Notably, taking a precession helix state with $\theta = \theta_0$ in Eq. (15) as the initial state, the evolved state is still a precession helix state but with varying $\theta(t) = \theta_0 + \int_0^t B_0(t')dt$. One finds that $|\psi(t)\rangle$ is a helix state at every fixed time point satisfying $\theta = n\pi + \pi/2$, $(n \in Z)$. Specifically, when we take $B_0(t)$ as a pulse field satisfying $B_0(t) = 0$ for $t > T$, and $\int_0^T B_0(t)dt = \pi/2$, we have a stable state with maximal helicity:

$$\mathbf{h}_l(t > T) = \tfrac{1}{2}[\sin(k_0 l), \cos(k_0 l), 0]. \quad (28)$$

As an example, we consider a Gaussian pulse driving field:

$$B_0(t) = \frac{\sqrt{\pi\alpha}}{2}\exp\left[-\alpha\left(t - \frac{T}{2}\right)^2\right], \quad (29)$$

where the internal T is taken sufficiently long as $\alpha \gg T^{-2}$ to meet $\int_0^T B_0(t)dt \approx \pi/2$. Note that the conclusion is obtained under the resonant condition $\Delta = 1$. It is expected that a similar helix state can still be obtained when Δ deviates a little from 1. The computation is performed by using a uniform mesh in the time discretization for the time-dependent Hamiltonian $H(t)$. We consider the case with initial state $|\psi(0)\rangle = |\phi(0)\rangle$. We introduce the quantity:

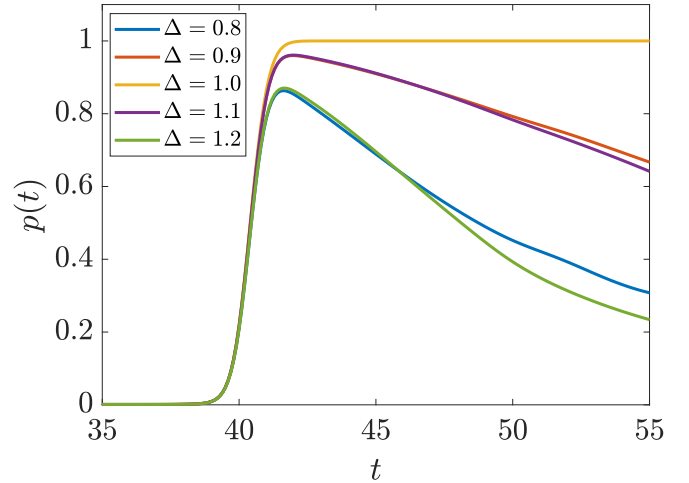$$p(t) = |\langle\psi(t)|\phi(\theta)\rangle|^2, \quad (30)$$

FIG. 2. Plots of the fidelity defined in Eq. (30) for the time evolution of initial ferromagnetic state under the Hamiltonian H with external field in Eq. (29) and different Δ. The target state is $|\phi(\pi/2)\rangle$, and the parameters are $\alpha = 0.5$, $T = 80$, $k_0 = \arctan(0.5)$, and $N = 10$. We find that (i) the fidelity reaches unity after the action of the pulsed field in the resonant case $\Delta = 1$, which accords with our analytical prediction; (ii) when $\Delta = 1 \pm 0.1$, the fidelity reaches a maximum close to unity; (iii) as Δ departs from 1, the maximum decreases but is still >0.8. The time is in units of J^{-1}, where J is the scale of the Hamiltonian, and we take $J = 1$.

to characterize the fidelity of the scheme. The plots of $p(t)$ in Fig. 2 for several typical cases show that the scheme works well even for the case with $\Delta \neq 1$. However, the flaw of this scheme is that the prior knowledge of system parameter k_0 and a time-dependent field is required, which motivates us to consider the non-Hermitian field that is independent of parameters of the system and time.

B. Non-Hermitian field

Now we turn to an alternative scheme to prepare a helix state by non-Hermitian H_I. It is a crossover scheme for the case that k_0 is unknown. We start with the investigation for an exactly solvable case, in which the external field is a complex spatially modulated field:

$$\mathbf{B}_j = B_0 \exp(ik_0 j)(1, i, 0), \quad (31)$$

with which we still have $[H_0, H_I] = 0$. Importantly, we have

$$H_I|\psi_n\rangle = B_0\sqrt{(n+1)(N-n)}|\psi_{n+1}\rangle, \quad (32)$$

with $n \in [0, N-1]$, which ensures the existence of an invariant $(N+1)$-D subspace spanned by a set of states $\{|\psi_n\rangle\}$. The matrix representation of Hamiltonian H is an $(N+1) \times (N+1)$ matrix M with nonzero matrix elements:

$$(M)_{N+1-n,N-n} = B_0\sqrt{(n+1)(N-n)}, \quad (33)$$

with $n = [0, N-1]$, and

$$(M)_{N+1-n,N+1-n} = -\frac{N-1}{4}, \quad (34)$$

with $n = [0, N]$. It is obvious $M + (N-1)/4$ is a nilpotent matrix, i.e.,

$$\left[M + \frac{N-1}{4}\right]^{N+1} = 0, \qquad (35)$$

or an $(N+1)$-order Jordan block. The dynamics for any states in this subspace is governed by the time evolution operator:

$$U(t) = \exp(-iMt) = \sum_{l=0}^{N} \frac{1}{l!}(-iMt)^l. \qquad (36)$$

Then for the initial state $|\psi(0)\rangle = |\Downarrow\rangle$, we have the normalized evolved state:

$$|\psi(t)\rangle = \frac{\exp\left[it\frac{N-1}{4}\right]}{\sqrt{\left(1 + B_0^2 t^2\right)^N}} \prod_{j=1}^{N}[-itB_0 \exp(ik_0 j)|\uparrow\rangle_j + |\downarrow\rangle_j], \qquad (37)$$

which turns to the coalescing state, i.e., $|\psi(\infty)\rangle \longrightarrow |\Uparrow\rangle$. Accordingly, we have

$$\mathbf{h}_l(t) = \frac{B_0 t}{1 + B_0^2 t^2}\left[\sin(k_0 l), \cos(k_0 l), \frac{B_0^2 t^2 - 1}{2B_0 t}\right], \qquad (38)$$

which indicates that $|\psi(t)\rangle$ is a helix state at finite time. At instant $t = B_0^{-1}$, it reaches the maximal helicity:

$$\mathbf{h}_l(B_0^{-1}) = \tfrac{1}{2}[\sin(k_0 l), \cos(k_0 l), 0]. \qquad (39)$$

The above analysis is still true when we take $\mathbf{B}_j = B_0 \exp(-ik_0 j)(1, -i, 0)$ and $|\psi(0)\rangle = |\Uparrow\rangle$, which corresponds to a time-reversal process.

C. Non-Hermitian boundary

So far, it seems that the introduction of the complex field does not improve the scheme since it still requires a specific field distribution. The only difference is that the time evolution under $U(t)$ is unidirectional, rather than periodic in the Hermitian system. However, there is a key fact that the Jordan block still exists when we take a local complex field at lth site:

$$\mathbf{B}_j = B_0 \delta_{jl}(1, i, 0). \qquad (40)$$

In the case of $\Delta \neq 1$, states $|\Downarrow\rangle$ and $|\Uparrow\rangle$ are two degenerate states of the Hermitian Hamiltonian H_0, and we have

$$H|\Uparrow\rangle = -\frac{(N-1)\Delta}{4}|\Uparrow\rangle, H^\dagger|\Downarrow\rangle = -\frac{(N-1)\Delta}{4}|\Downarrow\rangle, \qquad (41)$$

due to the facts:

$$H_I|\Uparrow\rangle = 0, \quad (H_I)^\dagger|\Downarrow\rangle = 0. \qquad (42)$$

It means that two states $|\Downarrow\rangle$ and $|\Uparrow\rangle$ are mutually biorthogonal conjugate and $\langle\Downarrow|\Uparrow\rangle$ is the biorthogonal norm of them. Importantly, the vanishing norm $\langle\Downarrow|\Uparrow\rangle = 0$ indicates that state $|\Uparrow\rangle$ ($|\Downarrow\rangle$) is the coalescing state of H ($H^\dagger$), or Hamiltonians H and $H^\dagger$ get an EP. From the perspective of dynamics, we have

$$\exp(-iHt)|\Downarrow\rangle \longrightarrow |\Uparrow\rangle, \quad \exp(-iH^\dagger t)|\Uparrow\rangle \longrightarrow |\Downarrow\rangle, \qquad (43)$$

for a sufficiently long time t. Although both states $|\Downarrow\rangle$ and $|\Uparrow\rangle$ are not helix states, $\exp(-iHt)|\Downarrow\rangle$ and $\exp(-iH^\dagger t)|\Uparrow\rangle$ may

have helicity at finite t from the observation at the end of the previous subsection, for instance, Eq. (39).

This inspires us to consider a balanced local complex field:

$$\mathbf{B}_j = B_0[\delta_{1j}(1, i, 0) + \delta_{Nj}(1, -i, 0)], \qquad (44)$$

which acts as a non-Hermitian boundary and may result in a stable helix state after a relaxation time. The physical intuition for this setup is simple. One complex field acts as a source of spin flips, while the other one takes the role of a drain. It is expected that a stable helix state emerges when the source and drain are balanced. However, it is hard to get an exact solution in this case due to the fact $[H_0, H_I] \neq 0$. In the following, we investigate this issue by perturbation method. In the subspace spanned by the set of degenerate ground states $\{|\psi_n\rangle\}$ of H_0, the matrix representation of Hamiltonian H with $\Delta = 1$ is an $(N+1) \times (N+1)$ matrix $\mathcal{H}$ with nonzero matrix elements:

$$(\mathcal{H})_{N+1-n,N-n} = \frac{B_0 \exp(-ik_0)}{N}\sqrt{(n+1)(N-n)}, \quad (45)$$

$$(\mathcal{H})_{N-n,N+1-n} = \frac{B_0 \exp(ik_0 N)}{N}\sqrt{(n+1)(N-n)}, \quad (46)$$

with $n = [0, N-1]$, and

$$(\mathcal{H})_{N+1-n,N+1-n} = -\frac{N-1}{4}, \qquad (47)$$

with $n = [0, N]$. In small B_0 limit, the eigenvalues and eigenvectors of matrix $\mathcal{H}$ are the approximate solutions of the non-Hermitian Hamiltonian. We note that matrix $\mathcal{H}$ is essentially related to the representation of the Hamiltonian $\mathcal{H}'$ of a fictitious spin $S = N/2$ particle: $\mathcal{H}' = \lambda S_x$, where S_x is its angular momentum operator, and λ is some complex constant. Then the normalized approximate eigenstates can be obtained from states $\{|\psi_n\rangle\}$:

$$|\widetilde{\psi}_n\rangle = R|\psi_n\rangle = \prod_{j=1}^{N} R_j|\psi_n\rangle, \qquad (48)$$

by a local transformation on spin at each site:

$$R_j = \frac{1}{\sqrt{2}}\begin{bmatrix} \exp\left(ik_0\frac{2j-N-1}{2}\right) & 1 \\ 1 & -\exp\left(-ik_0\frac{2j-N-1}{2}\right) \end{bmatrix}. \qquad (49)$$

The corresponding eigenenergy is complex:

$$E_n = -\frac{N-1}{4} + \frac{B_0 \exp\left[ik_0\frac{N-1}{2}\right]}{N}(2n-N), \qquad (50)$$

with $n = [0, N]$, and its imaginary part is

$$\text{Im}(E_n) = \frac{B_0}{N}(2n-N)\sin\left[\frac{k_0(N-1)}{2}\right]. \qquad (51)$$

Unlike a Hermitian system, the imaginary part of the eigenenergy can amplify or reduce the corresponding amplitude of the eigenstate in the dynamic process. For the given initial state $|\psi(0)\rangle = |\Uparrow\rangle$, when the evolution time is long enough, the final state is the eigenstate of H with the maximum imaginary part of eigenenergy. The corresponding approximate

(a) ferromagnetic state   (b) random pure state   (c) mixed state
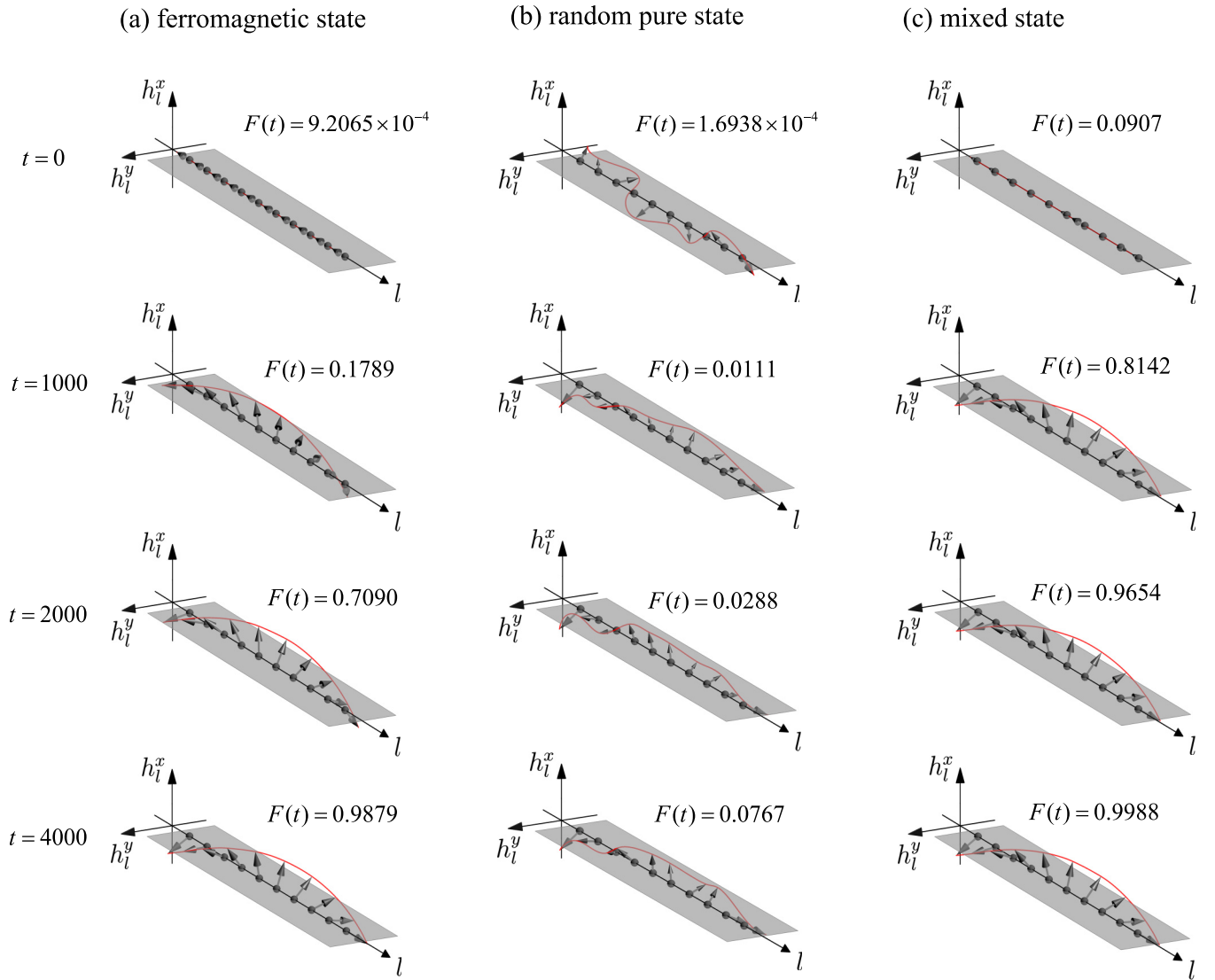

FIG. 3. Plots of numerical results of time evolution for three types initial states under the Hamiltonian H with non-Hermitian boundary in Eq. (44). The initial states are (a) ferromagnetic state, (b) pure random state, and (c) mixed state, which are defined in the text. The corresponding fidelity $F(t)$ defined in Eq. (60) is presented at several typical instants t. The complete plot of $F(t)$ is given in Fig. 4. The parameters are $B_0 = 0.005$, $N = 10$, and $k_0 = \arctan(0.5)$. It indicates that the evolved state for initial mixed state converges faster than that for the other two. The time is in units of J^{-1}, where J is the scale of the Hamiltonian, and we take $J = 1$.

eigenstate is

$$
|\psi(\infty)\rangle =
\begin{cases}
\displaystyle\sum_{n=0}^{N} p_n |\psi_n\rangle, & \sin\left[\frac{k_0(N-1)}{2}\right] > 0, \\
\displaystyle\sum_{n=0}^{N} (-1)^n p_n |\psi_n\rangle, & \sin\left[\frac{k_0(N-1)}{2}\right] < 0,
\end{cases}
\tag{52}
$$

where the coefficient is

$$
p_n = 2^{-N/2}\sqrt{C_N^n}\exp\left[-ik_0\frac{(N+1)n}{2}\right].
\tag{53}
$$

Accordingly, we have the helicity distribution along the chain:

$$
\mathbf{h}_l = \tfrac{1}{2}[\cos(k_0\ell), -\sin(k_0\ell), 0],
\tag{54}
$$

for $\sin[k_0(N-1)/2] > 0$, and

$$
\mathbf{h}_l = \tfrac{1}{2}[-\cos(k_0\ell), \sin(k_0\ell), 0],
\tag{55}
$$

for $\sin[k_0(N-1)/2] < 0$, where $\ell = l - (N+1)/2$ is a shifted coordinate. Obviously, the above two classes of state $|\psi(\infty)\rangle$ are standard helix states with opposite helicity due to the fact $|\mathbf{h}_l|^2 = 0.25$. The results in Eqs. (54) and (55) show the generated final state is a helix state with increasing azimuthal angle $k_0 = \arctan(D/J_x)$ under the resonant condition $\Delta = 1$. As we can see, k_0 increases as the strength of the DM interaction increases.

Numerical simulation is performed to verify our predictions. We compute the time evolution by exact diagonalization and present the dynamic process of the formation of the helix state through the time dependence of the helicity distribution $\mathbf{h}_l$. In general, the time evolution of an arbitrary initial state $\rho(0)$ obeys the equation:

$$
i\frac{\partial}{\partial t}\rho(t) = H\rho(t) - \rho(t)H^\dagger,
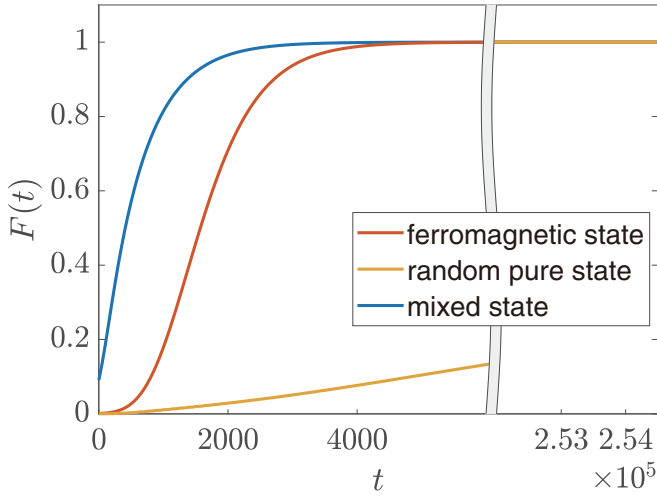\tag{56}
$$

FIG. 4. Plots of $F(t)$ in Eq. (60) as a function of time for the same time evolution process as in Fig. 3. We can see that the final states for three different initial states turn to the target state eventually. The time is in units of J^{-1}, where J is the scale of the Hamiltonian, and we take $J = 1$.

FIG. 5. Plots of helix vector of stable final state for different Δ. The initial state is $|\Downarrow\rangle$, and the parameters are $k_0 = \arctan(0.5)$, $B_0 = 0.005$, and $N = 10$.

which admits the formal solution:

$$\rho(t) = \exp(-iHt)\rho(0)\exp(iH^\dagger t). \quad (57)$$

Unlike the Hermitian case, the time evolution of the density matrix is no longer unitary. To get $\mathbf{h}_l(t)$, with the definition:

$$h_l^\alpha = \text{Tr}\big[\rho(t)s_l^\alpha\big], \quad (\alpha = x, y, z), \quad (58)$$

we normalize $\rho(t)$ by taking [39,40]

$$\rho(t) = \frac{\exp(-i\mathcal{H}t)\rho(0)\exp(i\mathcal{H}^\dagger t)}{\text{Tr}[\exp(-i\mathcal{H}t)\rho(0)\exp(i\mathcal{H}^\dagger t)]}, \quad (59)$$

in the following numerical calculation. We introduce the Uhlmann fidelity [41,42]:

$$F(t) = \left[\text{Tr}\sqrt{\sqrt{\rho_\text{h}}\rho(t)\sqrt{\rho_\text{h}}}\right]^2, \quad (60)$$

to characterize the degree of similarity between the evolved state $\rho(t)$ and the target state:

$$\rho_\text{h} = |\psi(\infty)\rangle\langle\psi(\infty)|. \quad (61)$$

The value of $F(t)$ after a sufficiently long time can be estimated intuitively. In general, an initial mixed state $\rho(0)$ contains equal-amplitude components in each state of $\{|\psi_n\rangle\}$. Then we always have $F(\infty) \approx 1$.

We focus on three types of initial states: (i) ferromagnetic state $\rho(0) = |\Downarrow\rangle\langle\Downarrow|$; (ii) random pure state $\rho(0) = |\psi(0)\rangle\langle\psi(0)|$, where

$$|\psi(0)\rangle = \left[\sum_{n=1}^{2^N}(\alpha_n)^2\right]^{-1/2}\sum_{n=1}^{2^N}\alpha_n|n\rangle. \quad (62)$$

Here, coefficient α_n is taken as a uniform random number within the interval $(-1, 1)$, and $\{|n\rangle\}$ is the complete set of eigenstates of H_0; and (iii) maximally mixed ferromagnetic
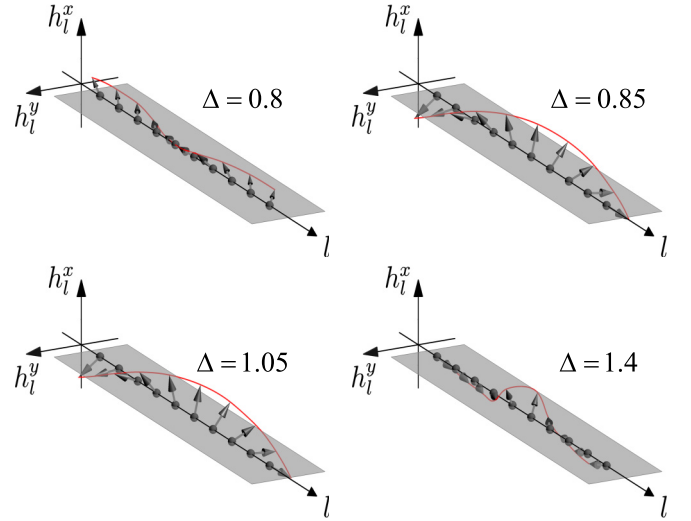
state:

$$\rho(0) = \frac{1}{N+1}\sum_{n=0}^{N}|\psi_n\rangle\langle\psi_n|. \quad (63)$$

The plots of $\mathbf{h}_l$ and $F(t)$ in Figs. 3 and 4 show the dynamic behaviors of the evolved states of the above three types of initial states, induced by the non-Hermitian boundary. It indicates that the evolved states for the initial mixed state and the ferromagnetic state converge rapidly. Importantly, the final states for all three different initial states turn to the target state after a sufficiently long time. The time evolution of the random pure initial state implies an arbitrary initial state will evolve into the eigenstate of H with the maximum imaginary part of eigenvalue after a sufficiently long time, and the steady final state is a standard helix state. Notably, the initial states, as well as the selected non-Hermitian boundary, do not contain any information of the prequench Hamiltonian.

Considering the system parameter Δ has a small deviation from resonant case with $\Delta = 1$, the strength of the DM interaction is equivalently changed when other parameters are fixed. Taking the saturated ferromagnetic state as the initial state, we investigate how the quench dynamics evolve numerically. The situation of the Hermitian external field is presented in Fig. 2; the evolved state first approaches the helix state and then deviates it. For the case of a balanced local non-Hermitian external field, the plots of the helix vector of the stable final state for several representative values of Δ are shown in Fig. 5. When the deviation of Δ is small, the stable final state is still a helix state but is the entangled one because we note that $|\mathbf{h}_l|^2 < \frac{1}{4}$. For a larger deviation of Δ, the stable final state is no longer a helix state.

V. SUMMARY

In summary, we have studied the possible helix states in the XXZ Heisenberg model with a DM interaction. Unlike the previous works on this topic, the existence of the spin helix state in this paper is the direct result of the resonant DM interaction. Our findings offer a method for the efficient preparation of a spin helix state as the ground state of a spin chain by the quench dynamic process with the aid of non-Hermitian balanced perturbation. It is expected to be insightful for quantum engineering by a non-Hermitian boundary. There are two merits to preparing a helix state through the method of the non-Hermitian field. One is that our method is independent of the initial state, i.e., taking an arbitrary state as the initial state, a steady helix state will be generated after a sufficiently long time under the driving of the balanced local non-Hermitian field. The other one is that the external field is local and is independent of the system parameters. Recently, the non-Hermitian quantum systems have been realized experimentally [43–47]. For instance, a non-Hermitian quantum many-body system has been achieved with ultracold atoms [47], which implies the feasibility of non-Hermitian methods in experiments; therefore, it is hopeful that our scheme will be realized experimentally in the near future.

[1] J. Zhang, G. Pagano, P. W. Hess, A. Kyprianidis, P. Becker, H. Kaplan, A. V. Gorshkov, Z. X. Gong, and C. Monroe, Observation of a many-body dynamical phase transition with a 53-qubit quantum simulator, Nature (London) **551**, 601 (2017).

[2] H. Bernien, S. Schwartz, A. Keesling, H. Levine, A. Omran, H. Pichler, S. Choi, A. S. Zibrov, M. Endres, M. Greiner *et al.*, Probing many-body dynamics on a 51-atom quantum simulator, Nature (London) **551**, 579 (2017).

[3] R. Barends, L. Lamata, J. Kelly, L. García-Álvarez, A. G. Fowler, A. Megrant, E. Jeffrey, T. C. White, D. Sank, J. Y. Mutus *et al.*, Digital quantum simulation of fermionic models with a superconducting circuit, Nat. Commun. **6**, 7654 (2015).

[4] E. J. Davis, A. Periwal, E. S. Cooper, G. Bentsen, S. J. Evered, K. Van Kirk, and M. H. Schleier-Smith, Protecting Spin Coherence in a Tunable Heisenberg Model, Phys. Rev. Lett. **125**, 060402 (2020).

[5] A. Signoles, T. Franz, R. Ferracini Alves, M. Gärttner, S. Whitlock, G. Zürn, and M. Weidemüller, Glassy Dynamics in a Disordered Heisenberg Quantum Spin System, Phys. Rev. X **11**, 011011 (2021).

[6] S. Trotzky, P. Cheinet, S. Fölling, M. Feld, U. Schnorrberger, A. M. Rey, A. Polkovnikov, E. A. Demler, M. D. Lukin, and I. Bloch, Time-resolved observation and control of superexchange interactions with ultracold atoms in optical lattices, Science **319**, 295 (2008).

[7] C. Gross and I. Bloch, Quantum simulations with ultracold atoms in optical lattices, Science **357**, 995 (2017).

[8] V. Popkov and C. Presilla, Obtaining pure steady states in nonequilibrium quantum systems with strong dissipative couplings, Phys. Rev. A **93**, 022111 (2016).

[9] V. Popkov and G. M. Schütz, Solution of the Lindblad equation for spin helix states, Phys. Rev. E **95**, 042128 (2017).

[10] V. Popkov, T. Prosen, and L. Zadnik, Exact Nonequilibrium Steady State of Open XXZ/XYZ Spin-$\frac{1}{2}$ Chain with Dirichlet Boundary Conditions, Phys. Rev. Lett. **124**, 160403 (2020).

[11] V. Popkov, X. Zhang, and A. Klümper, Phantom bethe excitations and spin helix eigenstates in integrable periodic and open spin chains, Phys. Rev. B **104**, L081410 (2021).

[12] P. N. Jepsen, J. Amato-Grill, I. Dimitrova, W. W. Ho, E. Demler, and W. Ketterle, Spin transport in a tunable Heisenberg model realized with ultracold atoms, Nature (London) **588**, 403 (2020).

[13] P. N. Jepsen, W. W. Ho, J. Amato-Grill, I. Dimitrova, E. Demler, and W. Ketterle, Transverse Spin Dynamics in the Anisotropic Heisenberg Model Realized with Ultracold Atoms, Phys. Rev. X **11**, 041054 (2021).

[14] S. Hild, T. Fukuhara, P. Schauß, J. Zeiher, M. Knap, E. Demler, I. Bloch, and C. Gross, Far-from-Equilibrium Spin Transport in Heisenberg Quantum Magnets, Phys. Rev. Lett. **113**, 147205 (2014).

[15] P. N. Jepsen, Y. K. Lee, H. Z. Lin, I. Dimitrova, Y. Margalit, W. W. Ho, and W. Ketterle, Long-lived phantom helix states in Heisenberg quantum magnets, Nat. Phys. **18**, 899 (2022).

[16] I. Dzyaloshinsky, A thermodynamic theory of "weak" ferromagnetism of antiferromagnetics, J. Phys. Chem. Solids **4**, 241 (1958).

[17] M. Bode, M. Heide, K. von Bergmann, P. Ferriani, S. Heinze, G. Bihlmayer, A. Kubetzka, O. Pietzsch, S. Blugel, and R. Wiesendanger, Chiral magnetic order at surfaces driven by inversion asymmetry, Nature (London) **447**, 190 (2007).

[18] U. K. Rößler, A. N. Bogdanov, and C. Pfleiderer, Spontaneous skyrmion ground states in magnetic metals, Nature (London) **442**, 797 (2006).

[19] K. Lee, R. Melendrez, A. Pal, and H. J. Changlani, Exact three-colored quantum scars from geometric frustration, Phys. Rev. B **101**, 241111(R) (2020).

[20] K. Lee, A. Pal, and H. J. Changlani, Frustration-induced emergent Hilbert space fragmentation, Phys. Rev. B **103**, 235133 (2021).

[21] R. F. Bishop, P. H. Y. Li, D. J. J. Farnell, and C. E. Campbell, Magnetic order in a spin-$\frac{1}{2}$ interpolating square-triangle Heisenberg antiferromagnet, Phys. Rev. B **79**, 174405 (2009).

[22] H. Y. Yuan, O. Gomonay, and M. Klaui, Skyrmions and multi-sublattice helical states in a frustrated chiral magnet, Phys. Rev. B **96**, 134415 (2017).

[23] O. I. Utesov and A. V. Syromyatnikov, Formation of spiral ordering by magnetic field in frustrated anisotropic antiferromagnets, Phys. Rev. B **100**, 054439 (2019).

[24] A. E. Koshelev, Phenomenological theory of the magnetic 90° helical state, Phys. Rev. B **105**, 094441 (2022).

[25] C. M. Bender, Making sense of non-Hermitian Hamiltonians, Rep. Prog. Phys. **70**, 947 (2007).

[26] N. Moiseyev, *Non-Hermitian Quantum Mechanics* (Cambridge University Press, Cambridge, 2011).

[27] A. Krasnok, D. Baranov, H. Li, M.-A. Miri, F. Monticone, and A. Alú, Anomalies in light scattering, Adv. Opt. Photon. **11**, 892 (2019).

[28] L. Feng, Y.-L. Xu, W. S. Fegadolli, M.-H. Lu, J. E. B. Oliveira, V. R. Almeida, Y.-F. Chen, and A. Scherer, Experimental demonstration of a unidirectional reflectionless parity-time metamaterial at optical frequencies, Nat. Mater. **12**, 108 (2013).

[29] S. K. Gupta, Y. Zou, X.-Y. Zhu, M.-H. Lu, L.-J. Zhang, X.-P. Liu, and Y.-F. Chen, Parity-time symmetry in non-Hermitian complex optical media, Adv. Mater. **32**, 1903639 (2019).

[30] A. Guo, G. J. Salamo, D. Duchesne, R. Morandotti, M. Volatier-Ravat, V. Aimez, G. A. Siviloglou, and D. N. Christodoulides, Observation of $\mathcal{PT}$-Symmetry Breaking in Complex Optical Potentials, Phys. Rev. Lett. **103**, 093902 (2009).

[31] C. E. Rüter, K. G. Makris, R. El-Ganainy, D. N. Christodoulides, M. Segev, and D. Kip, Observation of parity-time symmetry in optics, Nat. Phys. **6**, 192 (2010).

[32] B. Peng Ş. K. Özdemir, F. Lei, F. Monifi, M. Gianfreda, G. L. Long, S. Fan, F. Nori, C. M. Bender, and L. Yang, Parity-time-symmetric whispering-gallery microcavities, Nat. Phys. **10**, 394 (2014).

[33] L. Feng, Z. J. Wong, R.-M. Ma, Y. Wang, and X. Zhang, Single-mode laser by parity-time symmetry breaking, Science **346**, 972 (2014).

[34] H. Hodaei, M.-A. Miri, M. Heinrich, D. N. Christodoulides, and M. Khajavikhan, Parity-time-symmetric microring lasers, Science **346**, 975 (2014).

[35] L. Feng, R. El-Ganainy, and L. Ge, Non-Hermitian photonics based on parity-time symmetry, Nat. Photonics **11**, 752 (2017).

[36] K. L. Zhang and Z. Song, Resonant-amplified and invisible Bragg scattering based on spin coalescing modes, Phys. Rev. B **102**, 104309 (2020).

[37] X. Z. Zhang, L. Jin, and Z. Song, Dynamic magnetization in non-Hermitian quantum spin systems, Phys. Rev. B **101**, 224301 (2020).

[38] M. de Leeuw, C. Paletta, and B. Pozsgay, Constructing Integrable Lindblad Superoperators, Phys. Rev. Lett. **126**, 240403 (2021).

[39] D. C. Brody and E.-M. Graefe, Mixed-State Evolution in the Presence of Gain and Loss, Phys. Rev. Lett. **109**, 230405 (2012).

[40] K. Kawabata, Y. Ashida, and M. Ueda, Information Retrieval and Criticality in Parity-Time-Symmetric Systems, Phys. Rev. Lett. **119**, 190401 (2017).

[41] A. Uhlmann, The "transition probability" in the state space of a *-algebra, Rep. Math. Phys. **9**, 273 (1976).

[42] N. T. Jacobson, L. C. Venuti, and P. Zanardi, Unitary equilibration after a quantum quench of a thermal state, Phys. Rev. A **84**, 022115 (2011).

[43] Y. Wu, W. Liu, J. Geng, X. Song, X. Ye, C.-K. Duan, X. Rong, and J. Du, Observation of parity-time symmetry breaking in a single-spin system, Science **364**, 878 (2019).

[44] J. Li, A. K. Harter, J. Liu, L. de Melo, Y. N. Joglekar, and L. Luo, Observation of parity-time symmetry breaking transitions in a dissipative Floquet system of ultracold atoms, Nat. Commun. **10**, 855 (2019).

[45] M. Naghiloo, M. Abbasi, Yogesh N. Joglekar, and K. W. Murch, Quantum state tomography across the exceptional point in a single dissipative qubit, Nat. Phys. **15**, 1232 (2019).

[46] W. Liu, Y. Wu, C.-K. Duan, X. Rong, and J. Du, Dynamically Encircling an Exceptional Point in a Real Quantum System, Phys. Rev. Lett. **126**, 170506 (2021).

[47] Z. Ren, D. Liu, E. Zhao, C. He, K. K. Pak, J. Li, and G.-B. Jo, Chiral control of quantum states in non-Hermitian orbit-coupled fermions, Nat. Phys. **18**, 385 (2022).